Dalton Transactions

Cite this: *Dalton Trans.*, 2012, **41**, 5225

www.rsc.org/dalton

PAPER

Modelling the site of bromide binding in vanadate-dependent bromoperoxidases†

Verena Kraehmer and Dieter Rehder*

Received 29th November 2011, Accepted 15th February 2012
DOI: 10.1039/c2dt12287a

Treatment of Boc-protected (*S*)-serine (Ser) methyl ester with triphenylphosphine bromide Ph_3PBr (intermittently generated from PPh_3 and *N*-bromosuccinimide) yields Boc-3-bromoalanine (*R*)-Boc–BrAlaMe and, after deprotection, bromoalanine methyl ester (*R*)-BrAlaMe in the form of its hydrobromide. Boc–BrAlaMe and BrAlaMe have been structurally characterised. The reaction between BrAlaMe, salicylaldehyde (sal) and VO^{2+} results in the formation of Schiff base complexes of composition $[VO(sal–BrAlaMe)solv]^+$ (solv = CH_3OH: **3**, THF: **5**) and [VO(sal–BrAla)THF] **4**. DFT calculations of the structures of **3**, **4** and **5**, based on the B3LYP functional and employing the triple zeta basis set 6-311++g(d,p), provide distances Br···V = 4.0 ± 0.1 Å, if some distortion of the dihedral angle ∠N–C–C–Br is allowed (affording a maximum energy of *ca.* 45 kJ mol^{-1}), and thus model Br···V distances detected by X-ray methods in bromoperoxidases from the marine algae *Ascophyllum nodosum* and *Corallina pilulifera*. The DFT calculations have been validated by comparing calculated and found structures, including the new complex $[V^VO(Amp–sal)OMe(MeOH)]$ (**1**, Amp is the aminophenol moiety) and the known complex $[VO(L\text{-}Ser–van)H_2O]$ (van = vanillin). Additional validation has been undertaken by checking experimental against calculated (BHandHLYP) EPR spectroscopic hyperfine coupling constants. Complexes containing bromine as a substituent at the phenyl moiety of a Schiff base ligand do not allow for an appropriate simulation of the Br···V distance in peroxidases. The closest agreement, *d*(Br···V) = 4.87 Å, is achieved with [VO(3Br–salSer)THF] (**6**), where 3Brsal–Ser is the dianionic Schiff base formed between 3-Br-5-NO_2-salicylaldehyde and serine.

Introduction

Vanadate-dependent haloperoxidases are present in marine algae, terrestrial fungi and lichen. They contain vanadate O═V$(OH)_2O^-$ linked to the protein matrix *via* the N_ε of a histidine. The enzymes, and their functional mimics (*i.e.* specifically designed vanadium coordination compounds) catalyse the halogenation of organic substrates by reverting to halide, employing hydrogen peroxide as an oxidant.[1] Bromoperoxidases employ bromide; the brominating species generated by the oxidant, $\{Br^+\}$, can be Br_2, BrO^-/HOBr or Br_3^-. Structure information is available for the bromoperoxidases from the brown alga *Ascophyllum nodosum*,[2] and the red algae *Corallina officinalis*[3] and *Cor. pilulifera* (wild-type, and the mutant Arg397Trp).[4] The structure of the *Cor. pilulifera* enzyme in particular provides information on the location of bromide: Br^- resides close to the vanadate centre and interacts with Arg397 and other surrounding amino acids, including Ser483. Intermolecular contacts include Br···O(–V) = 3.6, Br···N(Arg) = 3.0, and (V–)O···Ser = 2.7 Å. In the *A. nodosum* enzyme, the respective amino acids are Arg349/480 and Ser416. In the solvent-exposed surface tyrosines of the bromoperoxidase from *Cor. pilulifera*, additional bromine has been found, which is covalently bonded to the phenyl moiety of tyrosine residues.[4] Mono- and dibrominated surface tyrosines have also been detected by EXAFS investigations in the *A. nodosum* bromoperoxidase.[5,6]

While bromination of tyrosine and other aromatic and pseudo-aromatic residues (such as phenylalanine and histidine) is easily achieved by electrophilic attack of a $\{Br^+\}$ species formed from Br^- and H_2O_2, the generation of an appropriate organic bromine species in the *absence* of peroxide is less straightforward. In previous studies based on XAS we have shown that in genuinely bromine-free *A. nodosum* bromoperoxidase, when soaked with bromide in the absence of peroxide, EXAFS features arise which can be fitted to a bromine–carbon distance *d*(Br–C) = 1.88 Å, a second sphere distance *d*(Br···C) = 2.67 Å, and a bromine–vanadium spacing *d*(Br···V) = 3.96–4.15 Å.[7–9] The range of *d* (Br–C) for Br bonded to an aromatic sp^2 carbon spans 1.88–1.92 Å,[6,9] that for *d*(Br–C) involving sp^3 carbons 1.92–1.96 Å,[6] extending to 1.87–1.99 Å for carbon in the β-position of an amide bond.[7a] In addition, steric constraints within

Chemistry Department, University of Hamburg, D-20147 Hamburg, Germany. E-mail: rehder@chemie.uni-hamburg.de

†Electronic supplementary information (ESI) available. CCDC 855090 (Boc–BrAlaMe) 855112 (BrAlaMe) and 855451 (**1**). For ESI and crystallographic data in CIF or other electronic format see DOI: 10.1039/c2dt12287a

the active site protein pocket are expected to give rise to unprecedented bond lengths variations. Although, on first sight, *d*(Br–C) = 1.88 Å more appropriately represents Br bonded to an aromatic framework, we have favoured – in the light of the unavailability of a $\{Br^+\}$ species and an electrophilic substitution path – linkage of bromine to an aliphatic carbon of one of the active site amino acids, and proposed serine (Ser416 in the *A. nodosum* enzyme) as a likely candidate.[7–9] Exchange of the OH^- for Br^- converts serine to bromoalanine, with Br residing on C_β.

Here, we provide evidence, based on a rational synthesis of (*R*)-β-bromoalanine (BrAla), for the enantioselective conversion of (active site) (*S*)-serine to BrAla. The oxidovanadium(IV) complexes of the Schiff base ligand formed between salicylaldehyde and BrAla are employed as model compounds to mimic active site Br···V distances under somewhat constrained conditions. In a second set of model complexes, Schiff bases obtained by condensation of serine or phenylalanine with salicylaldehydes brominated in the ring positions 3 or 6 are introduced. Structurally (by XRD) characterised Schiff base complexes have been employed to validate structure data obtained for complexes on the basis of DFT calculations, exemplified here for the complexes [VO(Amp–sal)(OMe)MeOH] **1** (Amp–sal is the Schiff base formed between aminophenol and salicylaldehyde; this work) and [VO(Ser–van)(H_2O)] **2** (Ser–van is the Schiff base formed between serine and vanillin).[10] The suitability of the B3LYP functional (employed in the current work) for predicting structure parameters and energies has recently been demonstrated for a an impressive number of transition metal complexes, including those of vanadium.[11] Complexes addressed in the present paper are collated in Schemes 1 and 2.

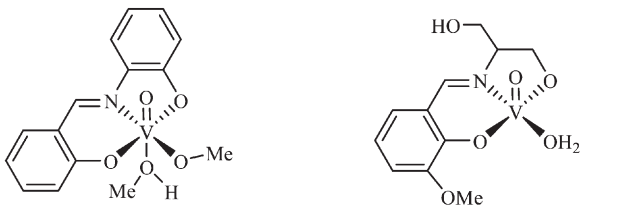

[VO(Amp-sal)(OMe)MeOH] **1** [VO(Ser-van)H_2O] **2**

Scheme 1 Structurally characterised Schiff base vanadium complexes chosen for the validation of structure data obtained from DFT calculations. For structure data of **2**, see ref. 10.

Results and discussion

Bromoalanine: preparation, characterisation and introduction into the coordination sphere of vanadium

In view of an unavailable rational synthesis for (*R*)-β-bromoalanine (BrAla) from (*S*)-serine (Ser) – the likely precursor for a putative BrAla at the enzyme's active site – we have devised a respective and efficient reaction course, Scheme 3. In a first step, the Boc-protected serine methyl ester Boc–SerMe (Boc = *tert*-butyloxycarbonyl) is prepared from serine methyl ester hydrochloride (SerMe) by deprotonation of SerMe with triethylamine (TEA) and concomitant reaction with Boc_2O.[12] The alcoholic function of serine is then replaced by bromine *via* treatment with triphenyl phosphine plus *N*-bromosuccinimide. In this so-called Mukaiyama redox condensation,[13] intermittently formed Ph_3PBr, containing the oxophilic Ph_3P moiety, is the actual brominating agent: nucleophilic attack of bromide to Boc–SerMe and concomitant formation of $Ph_3P{=}O$ yields the bromoalanine derivative Boc–BrAlaMe. Deprotection of Boc–AlaMe is then achieved with acetyl bromide in methanol. The bromoalanine methyl ester hydrobromide (BrAlaMe) thus formed can be converted to the neutral *N*-acetylated bromoalanine methyl ester Ac–BrAlaMe by treatment with acetyl bromide in methanol.[14]

The target compounds exhibit, in the EI-MS, the *m*/*z* peaks typical of the two bromine isotopomers (^{79}Br, ^{81}Br) at 281/283 ($[M]^+$) for Boc–BrAlaMe, 181/183 ($[M - HBr]^+$) for BrAlaMe, and 223/225 ($[M]^+$) for Ac–BrAlaMe. The ^{13}C DEPTQ NMR

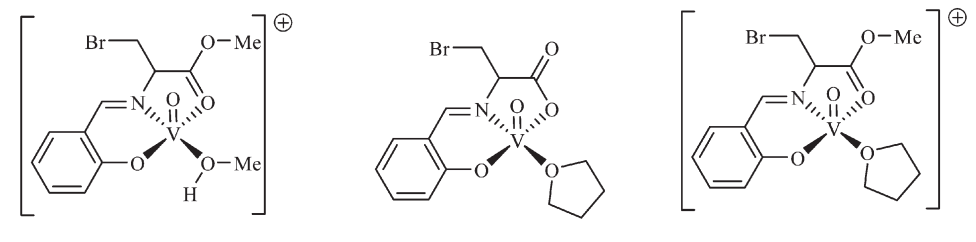

[VO(sal-BrAlaMe)MeOH]$^+$ **3** [VO(sal-BrAla)THF] **4** [VO(sal-BrAlaMe)THF]$^+$ **5**

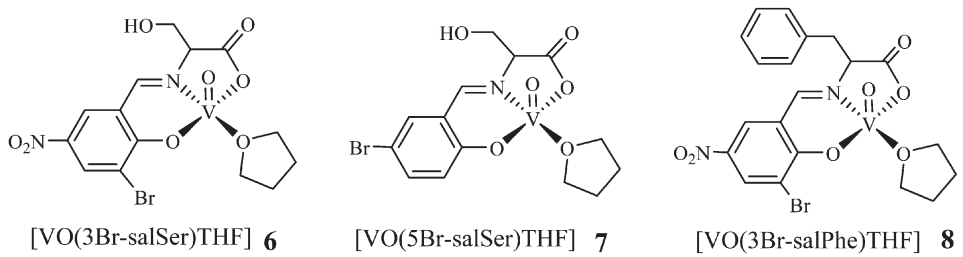

[VO(3Br-salSer)THF] **6** [VO(5Br-salSer)THF] **7** [VO(3Br-salPhe)THF] **8**

Scheme 2 Vanadium complexes with Schiff bases containing bromoalanine, serine or phenylalanine in the backbone. Counter-ion for the cationic complexes **3** and **5** is acetate.

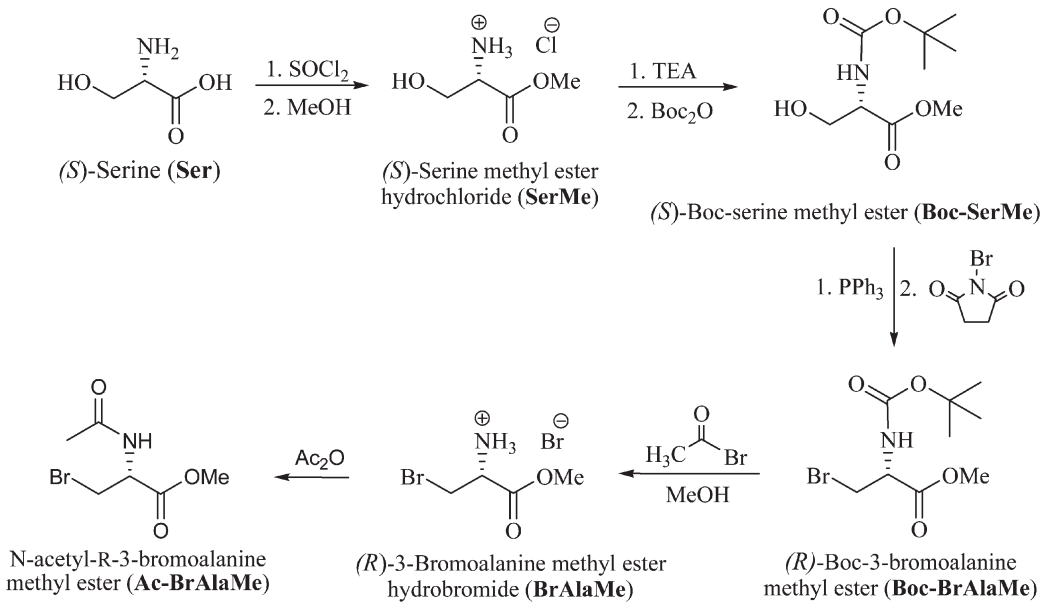

Scheme 3 The preparative route to bromoalanine derivatives. For details and abbreviations *cf.* text. Central step in this reaction course is the intermittent formation of Ph_3PBr, allowing for a conversion of Boc–SerMe to Boc–BrAlaMe.

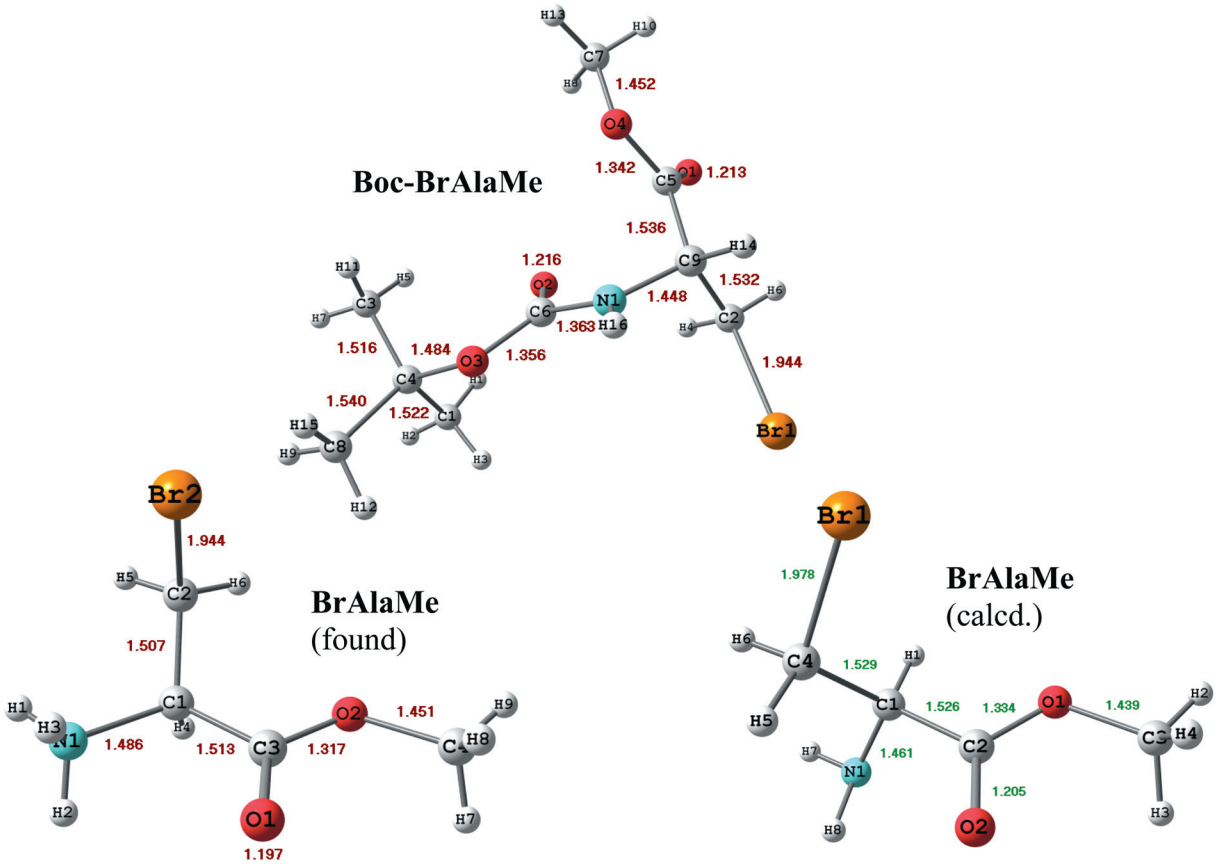

Fig. 1 Structures of the ligand precursors. See Scheme 3 for abbreviations. For BrAlaMe (counter-ion $Br^- \equiv$ Br1 omitted), the calculated structure is also shown.

signal for the methylene group carrying the bromo substituent appears at 30.1 ppm; the ν(C–Br) is at 590 (Boc–BrAlaMe), 591 (BrAlaMe) and 596 cm^{-1} (Ac–BrAlaMe), respectively. Boc–BrAlaMe and BrAlaMe have been characterised structurally by

Table 1 Selected bond lengths (Å) and angles (°) for bromoalanine derivatives

Boc–BrAlaMe found	BrAlaMe found	BrAlaMe calcd
Bond lengths	Bond lengths	Bond lengths
Br1–C2 1.944(4)	Br2–C2 1.944(3)	Br1–C4 1.986
N1–C9 1.448(6)	N1–C1 1.486(4)	N1–C1 1.464
O4–C5 1.342(5)	O2–C3 1.317(4)	O1–C2 1.335
O1–C5 1.213(5)	O1–C3 1.197(3)	O2–C2 1.206
Bond angles	Bond angles	Bond angles
Br1–C2–C9 110.0(3)	Br2–C2–C1 110.9(2)	Br1–C4–C1 112.95
N1–C9–C2 113.0(3)	N1–C1–C2 111.7(2)	N1–C1–C4 111.80
C5–C9–C2 108.4(3)	C3–C1–C2 113.1(3)	C2–C1–C4 110.37
Dihedral angles	Dihedral angles	Dihedral angles
H14–C9/C2–Br1 58.7	H4–C1/C2–Br2 −176.1	H1–C1/C4–Br1 −54.2
C5–C9/C2–Br1 175.1	C3–C1/C2–Br2 −56.0	C2–C1/C4–Br1 66.3
N1–C9/C5–O4 45.4	N1–C1/C3–O1 118.1	N1–C1/C2–O1 −178.8

XRD. Fig. 1 provides an overview of the structures, including the *calculated* structure for BrAlaMe, and Table 1 contains selected structure parameters. For crystal and refinement data see Experimental. The structure of the unprotected serine methyl ester (not shown in Fig. 1) has been published previously.[15]

Bond distances and bond angles for Boc–BrAlaMe and BrAlaMe are essentially identical, and the experimental bond distances and angles for BrAlaMe also agree with the calculated ones. On the other hand, the *dihedral* angles measured and calculated, respectively, for BrAlaMe clearly differ from each other in particular in the surroundings of the chiral centre C1: While the carbonyl group and nitrogen are in the same plane (∠O1C2–C1N1 = 179°) in the solid state structure, the respective angle in the calculated gas-phase structure is 118°. Further, the bromine substituent is in a plane perpendicular to the molecular axis defined by C1, C2 and O1 in the found structure, while the respective plane is twisted by 86° relative to this axis in the undisturbed, DFT-based structure. These differences, which reflect effects arising from the "salt-like" nature – four cationic BrAlaMe plus four Br^- counter ions in the unit cell – and packing effects in the crystal, minimise the requirement for space.

Oxidovanadium Schiff base complexes

Validation of calculated structure parameters. We have not succeeded in obtaining suitable crystals for the structure determination of vanadium complexes carrying ligands with bromine substituents, and resorted to DFT calculations for this reason. The calculations have been carried out with the B3LYP functional, employing the triple zeta basis set 6-311++g(d,p) (Gaussian 03). To validate these calculations, key data are compared with those obtained from X-ray diffraction studies of the new complex [V^VO(Amp–sal)OMe(MeOH)] (**1** in Scheme 1) and several Schiff base complexes with serine as a constituent, such as [V^{IV}O(Ser–van)H_2O] (**2** in Scheme 1), previously prepared in our laboratory.[10] We have further validated the calculated structures by comparing experimental EPR hyperfine coupling constants with those simulated (employing the program system BHandHLYP)[16a] on the basis of calculated bonding parameters.

The V^{IV} precursor compound [V^{IV}O(Amp–sal)THF] for the V^V complex **1** was prepared by the reaction between $VO(acac)_2$ (acac = acetylacetonate(1–)) and the Schiff base obtained from the condensation of aminophenol and salicylaldehyde in THF–methanol. Aerial oxidation of [V^{IV}O(Amp–sal)THF] in methanol results in the formation of **1**. An ORTEP plot of complex **1** is presented in Fig. 2 (top left). Found and calculated bonding parameters for **1** and **2** are provided in Table 2. Compound **1** crystallises in the space group $P2_1/n$. Vanadium constitutes a centre of chirality; the unit cell contains two pairs of the *C*/*A* enantiomers, Fig. 2, bottom left. Bond lengths for **1** are in the expected range. The rather long *d*(V–OHMe), 2.363(3) Å, is a consequence of the *trans* influence exerted by the oxido ligand, and has also been observed in other comparable complexes.[17] Larger deviations between calculated and observed bonding angles reflect influences impaired by packing effects in the crystal. As for **1**, bonding parameters obtained for the experimental structure of the serine derivative **2**[10] match those which have been calculated. Deviations in bond lengths amount to 0.03 Å at the most. The reliability of calculated bonding parameters in the case of compound **2** is supported by the close agreement (deviation 1.4%) between the calculated and experimental EPR spectroscopic parallel hyperfine constant: $|A_z|$ (calcd) = 167.7, $|A_z|$(found) = 170.1 × 10^{-4} cm^{-1}.

Complexes with BrAla in the coordination sphere. The complexes **3**, **4** and **5** (Scheme 2) have been synthesised in acetate-buffered solution from salicylaldehyde, BrAlaMe and vanadyl sulphate as depicted in eqn (1). Depending on the solvent, the cationic complex **3** (isolated from methanol–acetone) or the neutral complex **4** (isolated from methanol–THF) is recovered. In **3**, the bromoalanine moiety of the Schiff base ligand remains methylated and consequently coordinates through the carbonyl oxygen while, in the course of the formation of **4**, partial de-esterification occurs, allowing for coordination of the terminal carboxylate. In the ESI(+) and ESI(−) MS of the cationic complex **3**, the mass peaks 417/419 for [M − CH_3OH − H + VO]$^+$ and 283/285 [M − CH_3OH − H − VO]$^-$, respectively, are present, both deriving from the molecule (M = 383 g mol^{-1}).

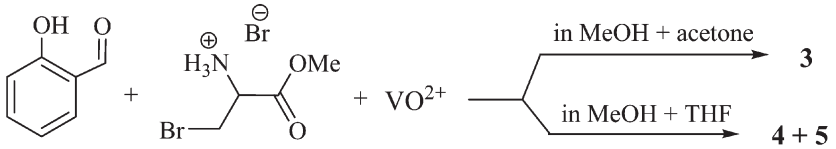

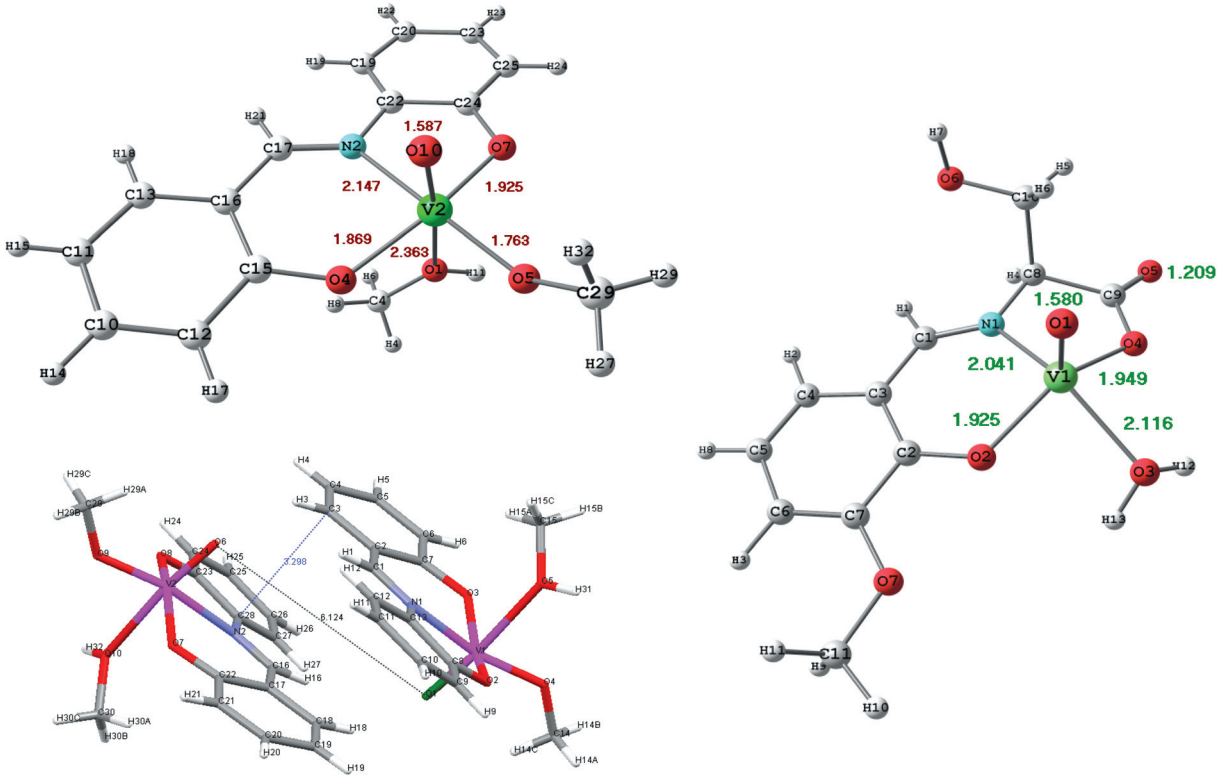

Fig. 2 Top left: Structure of the *C* enantiomer of [VO(Amp–sal)OMe(MeOH)], **1**. Bottom left: One of the two pairs of enantiomers present in the unit cell. Dashed lines indicate intermolecular contacts: The distance between the oxido ligands of the *A* and *C* enantiomers is 6.124 Å, the closest contact between phenyl carbons (belonging to sal and Amp, respectively, of the two enantiomers) amounts to 3.298 Å. Right: Calculated structure for [VO((*S*)-Ser–van)H_2O], **2** (for the X-ray structure see ref. 10).

Table 2 Found and calculated bond lengths (Å) and angles (°) for the Schiff base complexes [VO(Amp–sal)OMe(MeOH)] **1** and [VO((*S*)-Ser–van)H_2O] **2**

1	Found/calcd	**2**	Found[a]/calcd
V1–O5 [*d*(V=O)]	1.587(3)/1.572	V1–O1 [*d*(V=O)]	1.596(3)/1.580
V1–O4 [*d*(V–OAmp)]	1.925(3)/1.885	V1–O4 [*d*(V–Ocarb)][c]	1.972(3)/1.949
V1–O2 [*d*(V–Osal)]	1.869(3)/1.862	V1–O2 [*d*(V–Ovan)]	1.894(3)/1.925
V1–O3 [*d*(V–OMe)]	1.763(3)/1.759		
V1–O1 [*d*(V–OHMe)]	2.363(3)	V1–O3 [*d*(V–OH_2)]	1.979(3)/2.116
V1–N1	2.147(4)/2.225	V1–N1	2.022(3)/2.041
C6–O4 [*d*(V–Ophe][b]	1.347(5)/1.295	C9–O4 [*d*(C–Ocarb)][c]	1.302(4)/1.318
∠V1–O5/O4–O4/O1	100.474(14)/107.54	∠V1–O1–O2	109.76(7)/114.32
∠V1–O5/O2–O4/O3	102.294(15)/106.32	∠V1–O1–O3	108.55(7)/109.80
∠V1–O5/O3–O4/O2	99.080(14)/107.99	∠V1–O1–O4	107.85(7)/113.68
∠V1–O5/O4–N1	93.519(15)/93.72	∠O1–V1–N1	103.72(7)/105.73

[a] From ref. 10. [b] "phe" refers to the phenolate oxygen of the aminophenol moiety. [c] "carb" refers to the carboxylate oxygen of the serine moiety coordinating to vanadium.

Table 3 Calculated and experimental EPR spectroscopic hyperfine coupling constants ($\times 10^{-4}$ cm^{-1}) for the complexes **3**, **4** and **5** (*cf.* Scheme 2) plus minor components formed in the reaction represented by eqn (1)

Complex (equatorial functions)	$\lvert A_x\rvert$ calcd	$\lvert A_y\rvert$ calcd	$\lvert A_z\rvert$ calcd/found
3 (O_{phen}, N_{imine}, O_{ester}, $O_{methanol}$)	70.7	69.5	176.2/177.2
4 (O_{phen}, N_{imine}, $O_{carboxylate}$, O_{THF})	61.7	60.8	165.7/168.6
5 (O_{phen}, N_{imine}, O_{ester}, O_{THF})	67.6	65.2	171.7/171.1
$[VO(MeOH)_4]^{2+}$	75.0	74.9	182.2/180.6
$[VO(THF)_4]^{2+}$	61.7	67.7	177.8/179.2

The two peaks of about equal intensity represent the $^{79}Br/^{81}Br$ isotopomers. The FAB-MS spectrum for the neutral complex **4** exhibits a peak at 329 for $[M - Br]^+$. Along with **4**, an additional major product, the cationic complex **5**, plus a minor product of the likely composition $[VO(THF)_4]^{2+}$ are formed. A corresponding (*i.e.* solvent-derived) minor product, $[VO(MeOH)_4]^{2+}$, is also observed along with **3**. The composition of all of the complexes is rationalised on the basis of a comparison of the experimental with the expected (*viz.* calculated) EPR spectral parameters; Table 3.

The bond length *d*(Br–C) in the calculated structures compare to those which are commonly found in experimental structures.

In contrast, the distances *d*(V···Br) and *d*(O···Br) (where O is the oxido ligand) obtained from the calculated structures of **3**, **4** and **5** are longer by 20–25% than the corresponding distances found in bromoperoxidases treated with bromide; Table 4. In the calculated equilibrium structure of **4** (Fig. 3, left), the dihedral angle formed between the fragments Br–C12 and C13–N is −71.05°, and the distance *d*(V···Br) amounts to 5.02 Å. As this angle becomes narrower (Fig. 3, right), distances (Table 5) are realised which reproduce those found experimentally. The corresponding distortions of the dihedral angle in the native enzyme may be caused by constraints in the active site protein pocket; the additional energy afforded for such a distortion, *e.g.* 46.5 kJ mol^{-1} to adapt to a distance of 3.9 Å, is low.

Complexes with bromophenyl as constituent of the Schiff base ligand. Complexes **6**, and the complex cations **7** and **8** (Scheme 2), containing bromo substituents at the salicylaldehyde moiety of the ligand, have been considered here in order to evaluate the possibility of bromine activation by intermittent linkage of Br to a phenyl moiety, such as provided by Phe397 in the fungal *Curvularia inaequalis* peroxidase.[18] Following a literature procedure,[19] the complexes were prepared in a one-pot synthesis from brominated 5-nitrosalicylaldehyde, vanadyl sulphate and serine in methanol–THF as shown for compound **6** in eqn (2). Fig. 4 shows the calculated structure for **6**, and Table 6 summarises selected structure parameters involving the bromine substituent, and the EPR spectroscopic coupling constants.

The complexes display non-distorted tetragonal–pyramidal geometry with THF in one of the equatorial positions. The deviations between calculated and experimental EPR spectroscopic coupling constants are less than 2% in all three cases, indicating that the calculated gas phase structure and the structure of the

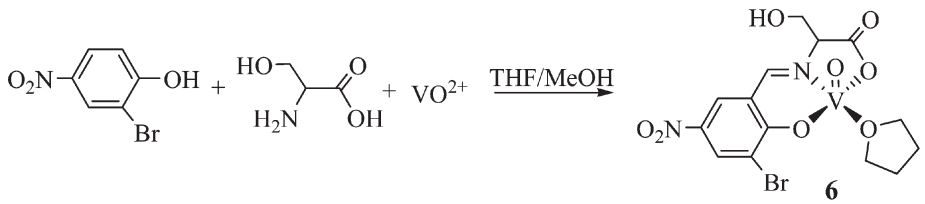

Table 4 Selected experimental and calculated equilibrium distances in Å

	Experimental in bromoperoxidases[a]	Calcd for the equilibrium dihedral angle ∠N–C/C–Br = −71.05°		
		3	**4**	**5**
d(C–Br)	1.87–1.99	1.959	1.984	1.960
d(V···Br)	3.6–4.1	5.009	5.020	5.008
d(O···Br)	3.6	4.844	4.840	4.813

[a] For refs. *cf.* Introduction.

Table 5 Non-equilibrium distances *d*(V···Br) of **4** and corresponding energies at constrained conditions

Dihedral angle ∠N–C/C–Br (°)	*d*(V···Br) (Å)	Energy difference relative to equilibrium state (kJ mol^{-1})
−71.0[a]	5.0	0
−24.0	4.1	32.9
−13.0	3.9	46.5
−2.0	3.7	57.6
+4.0	3.6	65.5

[a] Equilibrium state, *cf.* Fig. 3.

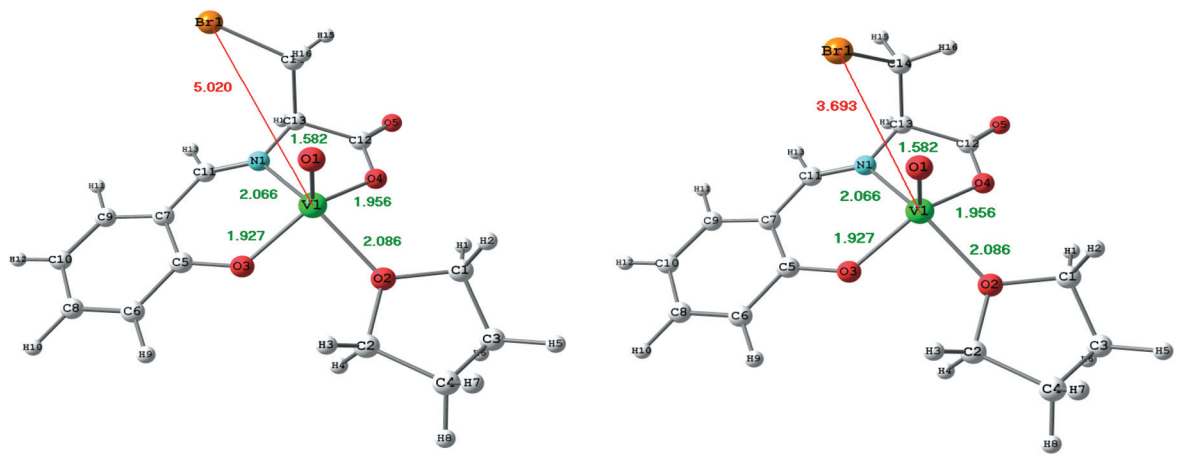

Fig. 3 Calculated structure of [VO(sal–BrAla)THF] (**4**) without (left) and with constraints (right). The dihedral angle Br–C13/C12–N is −71.0 (left) and −2.0° (right).

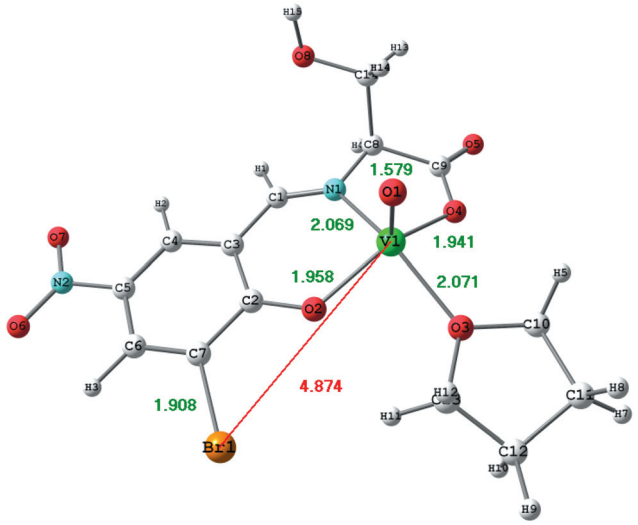

Fig. 4 Calculated gas-phase structure of [VO(3Br–salSer)THF] **6**, with the serinate moiety in the *S* and the vanadium centre in the *C* configuration. Selected bond lengths: V–O1 1.579, V–O2 1.958, V–O3 2.071, V–O4 1.941, V–N1 2.069, V1···Br1 4.874 (red line), O1···Br1 5.409 Å.

Table 6 Data (distances *d* in Å, EPR spectroscopic coupling constants (absolute values $|A|$ in 10^{-4} cm^{-1})) for complexes **6**, **7** and **8**

	d(C–Br)	*d*(Br···V)	*d*(Br···O)	A_x/A_y calcd	A_z calcd	A_x/A_y found	A_z found
6	1.907	4.874	5.409	64.7/62.8	168.3	62.8	171.3
7	1.918	7.508	7.979	59.9/57.9	166.1	57.9	168.5
8	1.908	4.872	5.432	63.4/62.1	168.3	61.2	171.3

compounds in solution are essentially identical. The closest available distance between the bromine substituent and the vanadium(IV) centre is 4.87 Å in **6** and **8**, *i.e.* in the complexes where Br is in the *meta* position with respect to the enamine linkage of the Schiff base. This distance exceeds that detected by X-ray methods of the enzymes soaked with bromide by approximately 0.9 Å; *cf.* Introduction for details and references.

Conclusion

We have shown that the Br···V distance of *ca.* 4 ± 0.1 Å found by X-ray methods in bromoperoxidases from the algae *Ascophyllum nodosum* and *Corallina pilulifera* can be modelled by oxidovanadium(IV) complexes of Schiff base ligands containing β-bromoalanine as a constituent, if some flexibility under constrained conditions is admitted. Schiff bases where the aromatic salicylaldehyde moiety is brominated are insufficiently flexible to allow for a satisfactorily close contact between vanadium and bromide. In the active site pocket, where serine (Ser416 in the *A. nodosum* enzyme) is directed towards the vanadium centre by virtue of the protein folding, a sufficiently close Br···V contact can be provided *per se*.

The strong electropositive potential at the bottom region of the active site cleft[4] may invoke bromide to the extent where the active site serine is converted to bromoalanine, a transformation which we have realised here through the conversion of serine to β-bromoalanine with triphenylphosphine + *N*-bromosuccinimide. Wever *et al.* have shown that, in the mutant Ser402Ala of the chloroperoxidase from the fungus *Curvularia inaequalis*, the brominating activity of the mutant enzyme decreases, although it still catalyses the oxidation of bromide.[18] The active sites of the chloro- and bromoperoxidases are very similar, the main difference being the substitution of a second histidine in the bromoperoxidase (His411) by a phenylalanine (Phe397) in the chloroperoxidase. In the light of the brominating activity of the Ser402Ala mutant of the *Cur. inaequalis* peroxidase, *i.e.* the sustenance of some brominating activity in the absence of serine suggests that active site residues other than – or in addition to – serine can become involved in bromide activation.

Experimental

General, instrumentation, and calculations

Where not mentioned otherwise (see syntheses of ligands and complexes), starting materials were obtained from commercial sources.

IR spectra: Perkin-Elmer FT-IR spectrometer 1720. ^{1}H NMR and ^{13}C NMR spectra: Bruker AVANCE 400 and Varian Gemini-200 BB. EPR spectra: X-band (9.35 MHz) Bruker Elexsys E500 CW at 120–100 K, *i.e.*, in glassy frozen solutions. The ^{51}V NMR was obtained on a Bruker AVANCE 400 spectrometer at 105.2 MHz, and is quoted relative to neat $VOCl_3$. FAB-MS: VG Analytical mass spectrometer 70–250S, employing argon for ionisation and *m*-nitrobenzyl alcohol as a matrix. ESI-MS: Finnigan ThermoQuest spectrometer, model MAT 95XL. MS spectra of organic compounds were obtained by electron impact ionisation with direct inlet. Polarimetry: Krüss polarimeter P8000. Crystal structures were performed with single crystals, embedded (under inert gas atmosphere) in viscous paraffin oil with Mo Kα irradiation (graphite monochromator) on a Bruker Smart Apex CCD diffractometer at 153 K. Frames were read with SAINT, absorption corrections were carried out with SADABS, and refinements with SHELXL 97.[20] All non-hydrogen atoms were refined with anisotropic temperature factors. Hydrogen atoms were either calculated into idealised positions, or found and refined isotropically. Table 7 summarises crystal structure data and refinement data, and also provides CCDCs.

DFT calculations have been carried out with the programme Gaussian 03[21] using the hybrid functional B3LYP[22] for geometry optimisation, and the basis set 6-311g++d,p (for complexes) and 6-311g++3d3p (for organic compounds). Based on this basis set and employing the half-and-half functional BHandHLYP, the isotropic EPR spectroscopic hyperfine coupling constants A_{iso} and the tensor components T_x, T_y, T_z were calculated.[16] The directional components of A were then calculated according to $A_n = A_{iso} + T_n$ ($n = x, y, z$), and are quoted as absolute values, $|A|$.

Table 7 Crystal and refinement data for Boc–BrAlaMe, BrAlaMe, and [VO(Amp–sal)OMe(MeOH)] (**1**)

	Boc–BrAlaMe	BrAlaMe	[VO(Amp–sal)OMe(MeOH)]
Empirical formula	$C_9H_{16}BrNO_4$	$C_4H_9Br_2NO_2$	$C_{15}H_{16}NO_5V$
M/g mol^{-1}	282.13	262.93	341.23
Crystal system, space group	Monoclinic, $P2_1$ (no. 4)	Orthorhombic, $P2_12_12_1$ (no. 19)	Monoclinic, $P2_1/n$ (no. 14)
a/pm	9.320(8)	5.253(8)	7.1797(17)
b/pm	5.102(8)	11.825(8)	21.233(5)
c/pm	13.905(10)	13.896(10)	19.471(5)
β/°	108.30(10)	—	99.801(5)
Z	2	4	8
V/Å^3	627.79(2)	863.17(2)	2925.0(12)
ρ_{calcd}/g cm^{-3}	1.493	2.023	1.550
μ/mm^{-1}	3.27	9.33	0.701
F(000)	288	504	1408
Crystal size/mm^3	0.40 × 0.10 × 0.10	0.50 × 0.07 × 0.07	0.50 × 0.07 × 0.07
θ range/°	2.30–27.48	2.30–25.00	1.92–27.00
Index range	$-7 < h < 11$, $-6 < k < 6$, $-18 < l < 17$	$-6 < h < 6$, $-15 < k < 15$, $-18 < l < 18$	$-9 < h < 8$, $-24 < k < 27$, $-24 < l < 17$
Reflections collected	4139	10 541	18 756
Independent reflections (R_{int})	2637 (0.0306)	1971 (0.0388)	6295 (0.0973)
R_1, wR_2 [$I < 2\sigma(I_0)$]	0.0393, 0.0921	0.0219, 0.0477	0.0581, 0.0950
R_1, wR_2 (all data)	0.0981, 0.1062	0.0241, 0.0477	0.1397, 0.1116
Residual electron density/e Å^{-3}	0.678 and −0.305	0.549 and −0.286	0.509 and −0.532
Flack parameter	0.0438	−0.0088	—
CCDC no.	855090	855112	855451

Syntheses of ligands and complexes

Esters of bromoalanine. Confer also Scheme 3. (1) (*S*)-Boc–serine methyl ester (Boc–SerMe): (*S*)-Serine methyl ester hydrochloride (SerMe) was prepared by treatment of (*S*)-serine with thionyl chloride in absolute methanol. Treatment of a suspension of SerMe in CH_2Cl_2 with triethyl amine, followed by bis(*tert*-butyl)dicarbonate (Boc_2O) yielded a viscous residue, from which Boc–SerMe was obtained by successive extractions with ethyl acetate, followed by aqueous 1 M $KHSO_4$, 1 M $NaHCO_3$ and saturated aqueous NaCl.

(2) Bromoalanine derivatives: (a) (*R*)-3-Boc–bromoalanine methyl ester (Boc–BrAlaMe): Boc–SerMe (17 g, 77.5 mmol) and triphenylphosphine (25.8 g, 98.5 mmol) were dissolved in 200 mL of abs. THF. The solution was cooled in an ice bath, and successively (within one hour) treated with *N*-bromosuccinimide (17.5 g, 98.5 mmol). The dark brown suspension was stirred overnight at room temp., filtered, and the filtrate evaporated to dryness. The residue was redissolved in hexane–ethylacetate 1 : 1, filtered, and the filtrate purified by passage through a column of silica gel 60 μm (elutant: hexane–ethylacetate 1 : 1). After removal of the solvents *in vacuo*, 19.6 g (89.5% yield) of light-brown, crystalline Boc–BrAlaMe was recovered. Anal. calc. for $C_9H_{16}BrNO_4$ (282.13): C, 38.31; H, 5.72; N, 4.96. Found: C, 38.11; H, 5.70; N 5.01%. IR (KBr, cm^{-1}): ν(N–H) 3390; ν(C–H) 2983; ν(C═O) (ester) 1716; ν(C═O) (carbamate); ν(C–Br) 619. ^{1}H NMR ($CDCl_3$) δ: 5.41 (NH, 1H, m); 4.72 (N–CH, 1H, m); 3.70 (O–CH_3 and CH_2, 5H, m); 1.43 (CH_3, 9H, s). ^{13}C NMR ($CDCl_3$) δ: 169.6 (O═C–O), 154.9 (N–C═O), 80.4 ($C(CH_3)_3$), 53.8 (CH), 52.8 (O–CH_3), 34.0 (CH_2Br), 28.2 ($C(CH_3)_3$). MS, m/z: 281 $[M]^+$; 224 $[M - C_2H_3O_2]^+$; 209 $[M - C_4H_9O]^+$; 181 $[M - C_5H_9O_2]^+$; 57 $[M - C_5H_7BrNO_4]^+$. Single crystals were obtained by slow evaporation of $CHCl_3$ solutions at room temp. For crystal and refinement data see Table 7.

(b) (*R*)-3-Bromoalanine methyl ester hydrobromide (BrAlaMe): Boc–BrAlaMe (10 g, 35.4 mmol), dissolved in 100 mL of abs. methanol, was treated dropwise during two hours with freshly distilled acetyl bromide (8.7 g, 70.9 mmol) and stirred at room temp. for three days. Vacuum removal of the solvent yielded a residue which was treated with 150 mL of abs. acetone. The colourless residue was filtered off, washed with acetone and dried *in vacuo*. Yield: 4.74 g (10.07 mmol; 51%) of colourless, amorphous BrAlaMe. IR (KBr, cm^{-1}): ν(N–H) 3474; ν(C–H) 2951;ν(C═O) (ester) 1746; ν(C–Br) 591. Anal. calc. for $C_4H_9Br_2NO_2$ (262.93): C, 18.27; H, 3.45; N, 5.33. Found: C, 18.32; H, 3.34; N, 5.21%. ^{1}H NMR (CD_3OD) δ: 8.70 (3H, NH_3^+, 3H, br s), 4.86 (HC–N, 1H, m), 3.88 (CH_2 and O–CH_3, 5H, m). ^{13}C NMR (CD_3OD) δ: 167.2 (O═C–O), 53.4 (C–N), 52.6 (O–CH_3), 30.72 (CH_2). MS, m/z: 181 $[M]^+$, 122 $[M - C_2H_3O_2]^+$. $[\alpha]_D$ (20 °C, CH_3OH) = +3°. Single crystals were obtained by slow evaporation of CH_3OH solutions at room temp. For crystal and refinement data see Table 7.

(c) *N*-Acetyl-(*R*)-3-bromoalanine methyl ester (Ac–BrAlaMe): BrAlaMe (1.1 g, 3.8 mmol) was dissolved in 10 mL of 0.1 M ammonium hydrogencarbonate (pH = 8) and treated dropwise with 50 mL of a mixture of acetanhydride–methanol 1 : 3. After 2 hours of stirring at room temp., the solvents were removed with a rotary evaporator to yield a yellowish liquid of Ac–BrAlaMe (0.77 g, 3.49 mmol = 93% yield). Anal. calc. for $C_6H_{10}BrNO_3$ (224.05): C, 32.16; H, 4.50; N, 6.25. Found: C, 32.30, H, 4.41; N, 6.21%. IR (KBr, cm^{-1}): ν(NH) 3436; ν(CH) 2972; ν(C═O) (ester) 1741; ν(C═O) (amide) 1673; ν(C–Br) 597. ^{1}H NMR ($CDCl_3$) δ: 8.25 (N–H, 1H, s), 4.86 (C–H, 1H, m), 3.91 (m, CH_2, 2H, m) 3.72 (O–CH_3, 3H, s), 1.92 (CH_3, 3H, s). ^{13}C NMR ($CDCl_3$) δ: 169.2 (O–C═O), 164.5 (N–C═O), 59.4 (CH), 54.5 (O–CH_3), 33.8 (CH_2), 25.2 (CH_3). MS, m/z: 223 $[M]^+$; 164 $[M - C_2H_3O_2]^+$; 122 $[M - 101]^+$.

Methanol-methoxido-oxido-{*N*-2-(salicylideneamino)phenolato}-vanadium(v), [VO(Amp–sal)OMe(MeOH)] (1). Vanadyl acetylacetonate (1.31 g, 4.72 mmol) and salicylideneaminophenol (1.00 g, 4.72 mmol) were dissolved in 50 mL of hot methanol. After 24 hours of stirring, the hot solution was filtered through glass wool to remove all black particles. Slow evaporation of the solvent yielded 1.33 g (3.91 mmol, 91% yield) of light-brown, crystalline **1**. Anal. calc. for $C_{15}H_{16}NO_5V$ (314.24): C, 52.80; H, 4.73; N, 4.0. Found: C, 52.71; H, 4.83; N, 4.02%. IR (KBr, cm^{-1}): ν(CH) 3038, 2917, 2831; ν(C═N) 1615; ν(C–C) 1442; ν(CO) 1296, 1146; ν(V═O) 982. ^{1}H NMR (CD_3OD) δ: 9.23 (x, 1H, s), 7.72 (1H, dd), 7.69 (1H, dd), 7.62 (1H, m), 7.32 (1H, m), 7.14 (1H, m), 6.99 (1H, d), 6.79 (1H, dd), 3.78

(CH_3OH, 1H, s), 3.48 (CH_3O^-, 3H, s), 3.32 (CH_3OH, 3H, s). ^{13}C NMR (CD_3OD) δ: 1614 (C═N); 160.5, 148.5, 144.6, 139.3, 134.9, 131.7, 131.1, 128.7, 122.2, 121.0, 118.1, 117.5 (12 × aromatic C); 53.6 (CH_3O^-), 52.0 (CH_3OH). ^{51}V NMR (CD_3OD) δ: −532.4. For crystal and refinement data, see Table 7.

[VO(sal–BrAlaMe)MeOH]$^+$ (3), [VO(sal–BrAla)THF] (4), and [VO(sal–BrAlaMe)THF]$^+$ (5). All operations were carried out in oxygen-free solvents. $VOSO_4{\cdot}5H_2O$ (**3**: 0.96 g, 3.80 mmol; **4** and **5**: 0.32 g, 1.27 mmol) and sodium acetate trihydrate (**3**: 1.29 g, 9.50 mmol; **4** and **5**: 0.43 g, 3.17 mmol) were dissolved in 50 mL of methanol and treated with salicylaldehyde (**3**: 0.46 g, 3.80 mmol; **4** and **5**: 0.16 g, 1.27 mmol) dissolved in 10 mL of THF. Green solutions were thus obtained. Drop-wise addition of bromoalanine methyl ester hydrochloride, BrAlaMe (**3**: 1.0 g, 3.80 mmol; **4** and **5**: 0.34 g, 1.27 mmol) dissolved in 20 mL of methanol, and stirring overnight at room temp. in the dark, yielded green suspensions, which were filtered under inert gas atmosphere. The compounds were recovered by evaporating the filtrates to dryness *in vacuo*. **3**, with acetate as the counter-ion, was recovered as a green amorphous solid with a yield of 90%. Anal. calc. for **3**$[CH_3CO_2]{\cdot}H_2O$ (461.16): C, 36.46; H, 4.37; N, 3.04. Found: C, 36.26; H, 4.30; N, 3.11%. For compounds **4** and **5**, the residue obtained after evaporation was re-dissolved in 50 mL of abs. THF and stirred under reflux overnight. After filtration and evaporation of the solvent, a mixture of **4** and **5** (counter-ion: acetate) was isolated in the form of a green amorphous solid. IR, EPR and ESI-MS data for **3** and **4** (the predominant component in the mix of **4** and **5**) are collated in Table 8. For EPR hyperfine coupling constants, see also Table 3.

Table 8 IR (cm^{-1}), EPR parameter ($|A|$ in 10^{-4} cm^{-1}) and MS data for **3** and **4**

	ν(C═N)	ν(V═O)	ν(C–Br)	$g_{iso}/g_{x,y}$, g_z	$A_{iso}/A_{x,y}$, A_z	MS *m*/*z*
3	1626	987	618	1.972/1.983, 1.952	93.1/61.3, 177.2	ESI(+): 283 and 285 [M − MeOH − 2H − VO]$^+$ ESI(−): 417 and 419 [M − MeOH − H + VO]$^-$
4[a]	1622	988	612	1.973/1.982, 1.951	92.1/61.0, 168.6	FAB: 329 [M − Br]$^+$

[a] ν(C═O) = 1596 cm^{-1}.

[VO(3Br–salSer)THF] (6), [VO(5Br–salSer)THF] (7), [VO(3Br–salPhe)THF] (8). General procedure: All operations were carried out in O_2-free solvents. 2 equivalents of sodium acetate trihydrate and one equivalent of the amino acid were dissolved in 50 mL of methanol, and swiftly treated with one equivalent of the respective salicylaldehyde dissolved in 30 mL of THF. To this solution, one equivalent of $VOSO_4{\cdot}5H_2O$ dissolved in 30 mL of methanol was added over a time span of 30 min, and the mixture stirred at room temp. for 24 hours. The grimy-green precipitate was filtered off under inert gas atmosphere and extracted with THF. The THF was then evaporated *in vacuo*, the residue washed three times with 20 mL of diethyl ether, and dried *in vacuo*. The complexes were recovered in the form of green, amorphous solids. Specific details are compiled in Table 9. Table 10 contains selected characteristic spectroscopic data.

Acknowledgements

Part of the work was funded by the German Research Foundation (DFG project no. RE 431/20). We thank Dr Eugenio Garribba, University of Sassari (Italy), for support in the calculations of EPR spectroscopic parameters.

Table 9 Sample weights of the starting products for the preparation of complexes **6**, **7** and **8**, and product yields

Complex	Amino acid[a] g (mol)	Br–sal[b] g (mol)	$NaAc{\cdot}3H_2O$ g (mol)	$VOSO_4{\cdot}5H_2O$ g (mol)	Yield
6	0.44 (4.19)	1.01 (4.11)	1.26 (8.28)	0.98 (4.13)	1.46 g (89%)
7	0.53 (5.14)	1.02 (5.07)	1.55 (10.19)	1.21 (5.10)	1.51 g (84%)
8	0.68 (4.12)	1.01 (4.11)	1.26 (8.28)	0.98 (4.13)	2.04 g (85%)

[a] (*S*)-Serine in the case of **6** and **7**, (*S*)-phenylalanine in the case of **8**. [b] **6** and **8**: 3-bromo-5-nitrosalicylaldehyde, **7**: 5-bromosalicylaldehyde.

Table 10 IR (cm^{-1}), EPR parameters ($|A|$ in 10^{-4} cm^{-1}) and FAB-MS data for **6**, **7** and **8**

	ν(C═N)	ν(C═O)	ν(V═O)	ν(CBr)	$g_{iso}/g_{x,y}$, g_z	$A_{iso}/A_{x,y}$, A_z	MS *m*/*z*
6[a]	1619	1587	982	1089	1.973/1.982, 1.948	98.1/62.8, 171.3	398 [M − THF + H]$^+$
7	1616	1578	984	1066	1.974/1.981, 1.949	94.8/57.9, 168.5	353 [M − THF + H]$^+$
8[a]	1615	1582	981	1092	1.974/1.980, 1.949	96.8/61.2, 171.3	458 [M − THF + H]$^+$

[a] The ν(N═O) appear at 1544 and 1342 for **6**, and at 1561 and 1349 cm^{-1} for **8**.

References

1 (*a*) D. Wischang, O. Brücher and J. Hartung, *Coord. Chem. Rev.*, 2011, **255**, 2204–2217; (*b*) D. Rehder, *Bioinorganic Vanadium Chemistry*, John Wiley & Sons, Chichester, 2008.
2 M. Weyand, H.-J. Hecht, M. Kieß, M.-F. Liaud, H. Vilter and D. Schomburg, *J. Mol. Biol.*, 1999, **293**, 595–611.
3 M. N. Isupov, A. R. Dalby, A. A. Brindley, Y. Izumi, T. Tanabe, G. N. Murshudov and J. A. Littlechild, *J. Mol. Biol.*, 2000, **299**, 1035–1049.
4 J. Littlechild, E. G. Rodriguez and M. Isupov, *J. Inorg. Biochem.*, 2009, **103**, 617–621.
5 M. C. Feiters, C. Leblanc, F. C. Küpper, W. Meyer-Klaucke, G. Michel and P. Potin, *J. Am. Chem. Soc.*, 2005, **127**, 15340–15341.
6 M. C. Feiters, F. C. Küpper and W. Meyer-Klaucke, *J. Synchrotron Radiat.*, 2005, **12**, 85–93.
7 (*a*) H. Dau, J. Dittmer, M. Epple, J. Hanss, E. Kiss, D. Rehder, C. Schulzke and H. Vilter, *FEBS Lett.*, 1999, **457**, 237–240; (*b*) D. Rehder, C. Schulzke, H. Dau, C. Meinke, J. Hanss and M. Epple, *J. Inorg. Biochem.*, 2000, **80**, 115–121.
8 D. Rehder and V. Kraehmer, *Medimond Int. Proc.*, EUROBIC 10, 2010, 73–76.
9 U. Christmann, H. Dau, M. Haumann, E. Kiss, P. Liebisch, D. Rehder, G. Santoni and C. Schulzke, *Dalton Trans.*, 2004, 2534–2540.
10 M. Ebel and D. Rehder, *Inorg. Chem.*, 2006, **45**, 7083–7090.
11 (*a*) G. Micera and E. Garribba, *Int. J. Quantum Chem.*, 2011, **111**, DOI: 10.1002/qua.23237 online preprint (*b*) V. A. Nikolakis, J. T. Tsalavoutis, M. Stylianou, E. Evgeniou, T. Jakusch, A. Melman, M. P. Sigalas, T. Kiss, A. D. Keramidas and T. A. Kabanos, *Inorg. Chem.*, 2008, **47**, 11698–11710.
12 O. Keller, W. E. Keller, G. V. Look and G. Versin, *Org. Synth.*, 1990, **7**, 70–76.
13 T. Mukaiyama, *Angew. Chem., Int. Ed.*, 2004, **43**, 5590–5614.
14 G. E. Reid, R. J. Simpson and R. A. J. O'Hair, *J. Am. Soc. Mass Spectrom.*, 1998, **9**, 945–956.
15 A. Schouten and M. Lutz, *Acta Crystallogr., Sect. E: Struct. Rep. Online*, 2009, **65**, o3026.
16 (*a*) G. Micera and E. Garribba, *Dalton Trans.*, 2009, 1914–1918; (*b*) G. Micera and E. Garribba, *J. Comput. Chem.*, 2011, **32**, 2822–2835.
17 R. Fulwood, H. Schmidt and D. Rehder, *J. Chem. Soc., Chem. Commun.*, 1995, 1443.
18 N. Tanaka, Z. Hasan and R. Wever, *Inorg. Chim. Acta*, 2003, **356**, 288–296.
19 J. Costa Pessoa, I. Cavaco, I. Correia, M. T. Duarte, R. D. Gillard, R. T. Henriques, F. J. Higes, C. Madeira and I. Tomaz, *Inorg. Chim. Acta*, 1999, **293**, 1–11.
20 G. M. Sheldrick, *SHELXL-97, Program for Crystal Structure Refinement*, University of Göttingen, Germany.
21 M. J. Frisch, G. W. Trucks, H. B. Schlegel, G. E. Scuseria, M. A. Robb, J. R. Cheeseman, J. A. Montgomery, Jr., T. Vreven, K. N. Kudin, J. C. Burant, J. M. Millam, S. S. Iyengar, J. Tomasi, V. Barone, B. Mennucci, M. Cossi, G. Scalmani, N. Rega, G. A. Petersson, H. Nakatsuji, M. Hada, M. Ehara, K. Toyota, R. Fukuda, J. Hasegawa, M. Ishida, T. Nakajima, Y. Honda, O. Kitao, H. Nakai, M. Klene, X. Li, J. E. Knox, H. P. Hratchian, J. B. Cross, V. Bakken, C. Adamo, J. Jaramillo, R. Gomperts, R. E. Stratmann, O. Yazyev, A. J. Austin, R. Cammi, C. Pomelli, J. Ochterski, P. Y. Ayala, K. Morokuma, G. A. Voth, P. Salvador, J. J. Dannenberg, V. G. Zakrzewski, S. Dapprich, A. D. Daniels, M. C. Strain, O. Farkas, D. K. Malick, A. D. Rabuck, K. Raghavachari, J. B. Foresman, J. V. Ortiz, Q. Cui, A. G. Baboul, S. Clifford, J. Cioslowski, B. B. Stefanov, G. Liu, A. Liashenko, P. Piskorz, I. Komaromi, R. L. Martin, D. J. Fox, T. Keith, M. A. Al-Laham, C. Y. Peng, A. Nanayakkara, M. Challacombe, P. M. W. Gill, B. G. Johnson, W. Chen, M. W. Wong, C. Gonzalez and J. A. Pople, *GAUSSIAN 03 (Revision C.02)*, Gaussian, Inc., Wallingford, CT, 2004.
22 (*a*) A. D. Becke, *Phys. Rev. A: At., Mol., Opt. Phys.*, 1988, **38**, 3098–3100; (*b*) C. Lee, W. Yang and R. G. Parr, *Phys. Rev. B*, 1988, **37**, 785–789.

